Natural Resources Canada | Ressources naturelles Canada

GEOLOGICAL SURVEY OF CANADA
OPEN FILE 8430

High cerium anomalies in zircon from intrusions associated with porphyry copper mineralization in the Gibraltar deposit, south-central British Columbia

C.H. Kobylinski, K. Hattori, S.W. Smith, and A. Plouffe

2018

Canada

GEOLOGICAL SURVEY OF CANADA
OPEN FILE 8430

High cerium anomalies in zircon from intrusions associated with porphyry copper mineralization in the Gibraltar deposit, south-central British Columbia

C.H. Kobylinski[1], K. Hattori[1], S.W. Smith[2], and A. Plouffe[3]

[1] Department of Earth and Environmental Sciences, University of Ottawa, 25 Templeton Street, Ottawa, Ontario
[2] Taseko Gibraltar, 10251 Gibraltar Mine Road, McLeese Lake, British Columbia
[3] Geological Survey of Canada, 601 Booth Street, Ottawa, Ontario

2018

Permanent link: https://doi.org/10.4095/311194

This publication is available for free download through GEOSCAN (http://geoscan.nrcan.gc.ca/).

Recommended citation
Kobylinski, C.H., Hattori, K., Smith, S.W., and Plouffe, A., 2018. High cerium anomalies in zircon from intrusions associated with porphyry copper mineralization in the Gibraltar deposit, south-central British Columbia; Geological Survey of Canada, Open File 8430, 1 .zip file. https://doi.org/10.4095/311194

Publications in this series have not been edited; they are released as submitted by the author.

High cerium anomalies in zircon from intrusions associated with porphyry copper mineralization in the Gibraltar deposit, south-central British Columbia

Christopher H. Kobylinski[1], Keiko Hattori[1], Scott W. Smith[2], and Alain Plouffe[3]

[1] *Department of Earth and Environmental Sciences, University of Ottawa, 25 Templeton St., Ottawa, ON K1N 6N5*

[2] *Taseko Gibraltar, 10251 Gibraltar Mine Rd., McLeese Lake, British Columbia, V0L 1P0*

[3] *Geological Survey of Canada, 601 Booth Street, Ottawa, ON K1A 0E8*

Abstract: The Gibraltar porphyry-Cu deposit in the Quesnel Terrane in south-central British Columbia is hosted by the Late Triassic to Early Jurassic Granite Mountain Batholith (GMB). The GMB has been classified into four phases of tonalitic rocks with minor quartz diorite. The rocks of the Mine Phase, host of the Cu mineralization, are foliated tonalite and are extensively altered to form K-feldspar, white mica, epidote and pyrite. All zircon grains examined from the GMB are magmatic with Th/U ranging from 0.15 to 1.44 and low Nd/Yb ratios below 0.01. U-Pb dating of zircons reveals three Cu-mineralized intrusions within the Mine Phase ranging from 201 to 219 Ma. The age gaps between the mineralized intrusions are larger than the uncertainty of the age data. Zircons from the oldest Cu- mineralized intrusion (218.9±3.1 Ma) in the Mine Phase record the highest Ce^{4+}/Ce^{3+} (680± 180 (1 σ), n=14). Zircons from the two other groups of Cu-mineralized intrusions in the Mine Phase show lower Ce^{4+}/Ce^{3+} (214± 64 (1σ), n=43) and those from the unmineralized Border and Granite Mountain phases of the GMB show even lower Ce^{4+}/Ce^{3+} (128± 35 (1σ), n=108). Zircons from the Cretaceous Sheridan Creek Stock, south of the GMB, show low Ce^{4+}/Ce^{3+} (203± 60 (1σ), n=28). The data suggest multiple pulses of intrusions and mineralization in the Mine Phase, which is supported by Re-Os ages of molybdenite which are similar to the second and third pulses of intrusions. Ages and Ce^{4+}/Ce^{3+} values for zircons from Cu-mineralized rocks in the Mine Phase are similar to the values for intrusions associated with the Highland Valley porphyry Cu deposit in the Guichon Creek Batholith. The ratios Ce/Nd and Ce/Ce* from the measured concentrations of Ce, Nd, and Sm correlate well with Ce^{4+}/Ce^{3+}, based on the compositions of zircon and bulk rocks. This suggests that the compositions of detrital zircons in glacial sediments and streams may be used in mineral exploration to detect intrusions with affinity to host porphyry Cu mineralization.

Introduction

Previous studies show a strong correlation between the rare earth element composition of magmatic zircon and the oxidation state of the host intrusion (Ballard et al, 2002; Liang et al., 2006; Dilles et al., 2015; Shen et al., 2015; Lu et al., 2016; Lee et al., 2017). They further indicate a positive correlation between the oxidized nature of the intrusion recorded in the zircon composition with porphyry mineralization. Consequently, the study of magmatic zircons in the various intrusive phases of a batholith makes a two-fold contribution: geochronology and fertility potential of the magmas to generate ore fluids that produce porphyry mineralization.

We present new data on the composition and dating of zircon from the Granite Mountain Batholith (GMB) which is host of the 1.011 M tons (0.25% Cu; 0.008% Mo) porphyry Cu-Mo Gibraltar deposit (https://www.tasekomines.com/properties/gibraltar/reserves-and-resources). We show that the Mine phase, host of the mineralization, consists of three previously unrecognized pulses of intrusion that are more oxidized than the rest of the batholith

supporting the interpretation that porphyry deposits are associated with oxidized intrusion.

Granite Mountain batholith

The GMB is located in south-central British Columbia. It intrudes the Nicola Group mafic volcaniclastic rocks of the Quesnel terrane close to the contact with the Cache Creek terrane to the west (Schiarizza, 2015). It is host to the Gibraltar Cu-Mo porphyry deposit operated by Taseko Mines Ltd. Geological mapping in the region of the GMB and the setting of the deposit are reported by Sutherland Brown (1976), Drummond et al. (1976), Panteleyev (1978), Ash et al. (1999a, b), Bysouth et al. (1995), Ash and Riveros (2001), van Straaten et al. (2013), and Schiarizza (2014, 2015). Kobylinski et al. (2016; 2017) conducted an investigation of the assemblage minerals, texture and alteration of the GMB.

Intrusive phases and geochronology

The GMB is composed of tonalitic rocks with minor quartz diorite. Based on texture and mineralogy, it is divided into four intrusive phases including from west to east: Border phase (quartz diorite), Mine phase (tonalite), Granite Mountain phase (leucocratic tonalite), and the Burgess Creek stock (leucocratic tonalite) (Bysouth et al., 1995; Schiarizza, 2015) (Fig.1). Zircon U-Pb geochronology was previously reported for all phases except the Border phase.

In 2014, R. Friedman at the University of British Columbia completed two U-Pb zircon ages on the Burgess Creek stock (Schiarizza, 2015). One U-Pb age of 222.71±0.22 Ma was reported from leucocratic tonalite in the northwest margin of the stock and one age of 221.25±0.2 Ma for a quartz diorite 350 m southwest of the leucocratic tonalite. The age of the tonalite is older than the quartz

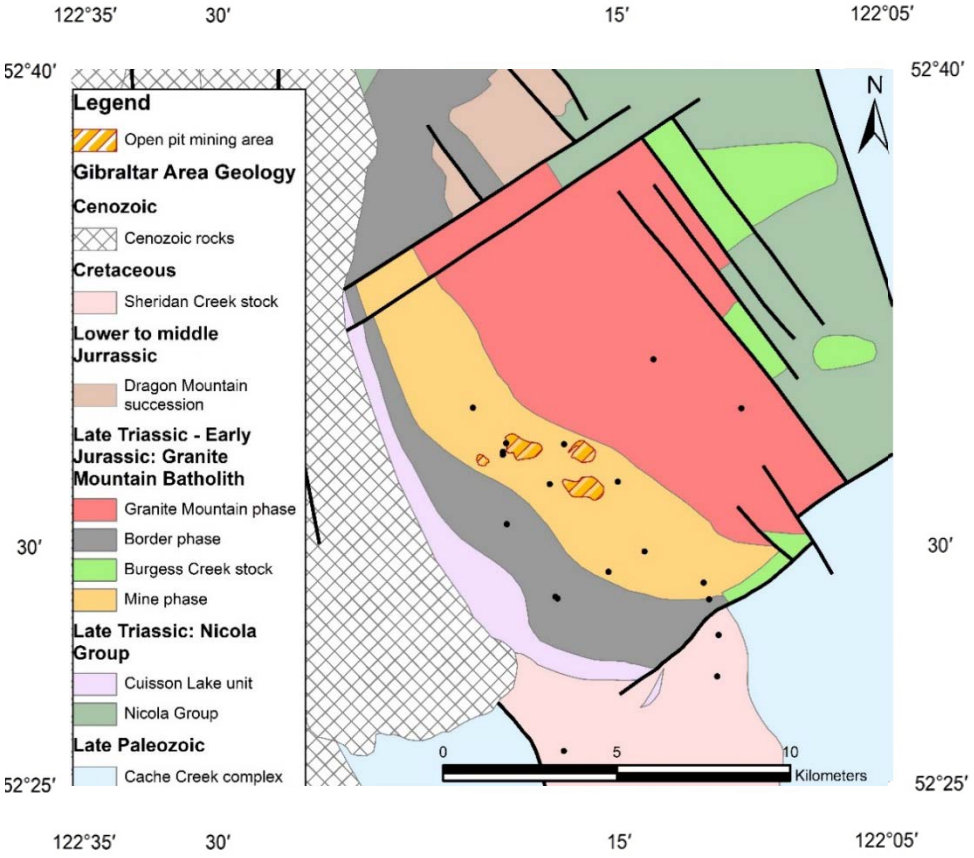

Figure 1. *Simplified geological map of the study area, modified from Plouffe and Ferbey (2015). Names of the phases and units taken from Schiarizza (2015). Small solid circles show locations of samples for this study.*

diorite, but tonalite also cross cuts quartz diorite, suggesting multiple injections of tonalitic magmas in the Burgess Creek stock (Schiarizza, 2015) (Figs. 1 and 2).

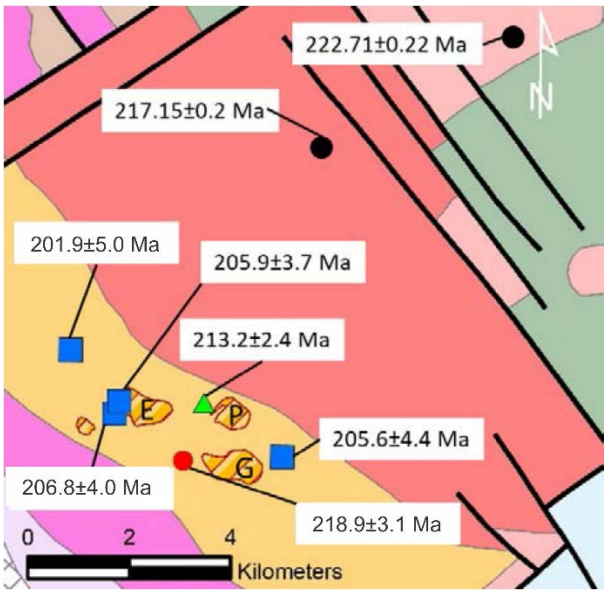

Figure 2. *Geological map of the GMB showing the locations of open pits and samples for U-Pb zircon dating. The locations of samples for U-Pb zircon dating by Friedman in 2014 cited by Schiarizza (2015) are shown as solid black circles. Locations of samples: Sample GBR-7 (red solid circle, 218.9±3.1 Ma), GBR-21 (blue solid square at 205.6±4.4Ma), GBR-2 (green solid triangle at 213.2±2.4 Ma), GBR-12(blue solid square at 206.8±4.0 Ma), GBR-15 (blue solid square at 205.9±3.7 Ma) and GBR-16 (blue solid square at 201.9±5.0 Ma). Open pits are the Gibraltar East pit (E), Polyanna pit (P) and Granite Lake pit (G).*

Zircon U-Pb ages were reported from two samples of the Granite Mountain phase. A sample just west of the Burgess Creek stock yielded an age of 217.15±0.2 Ma (by R. Friedman in 2014 at UBC; Schiarizza, 2015) (Figs. 1 and 2). Ash et al. (1999) reported a U-Pb zircon age of 215±0.8 Ma from tonalite in the Granite Mountain phase approximately 1.5 km north east of the Gibraltar mill site.

The Mine phase hosts the bulk of the porphyry Cu-Mo mineralization of the Gibraltar deposit. The Mine phase is over 13 km long and 3 km wide (Fig. 1). Oliver et al. (2009) report a U-Pb zircon laser ablation age of 211.9 ±4.3 Ma on a Mine phase tonalite (cf. Schiarizza, 2015).

The Sheridan Creek stock located south of the GMB has yielded a U-Pb zircon age of 108.1±0.6 Ma (Ash and Riveros, 2001).

Mineralization

Copper mineralization at Gibraltar occurs primarily as disseminated and veined chalcopyrite in the central part the Mine phase. Molybdenite occurs in quartz veins spatially associated with the Cu-mineralization. Re-Os ages on molybdenite reported by Harding (2012) range from 210.01±0.9 Ma to 215±1 Ma. Mineralization is associated with potassic alteration forming K-feldspar after plagioclase, and white mica alteration. The occurrence of chalcopyrite is associated with white mica which forms veins and replaces plagioclase (up to 30% replacement). Epidote is common in all rocks of GMB (Kobylinski et al., 2017). It forms veins and replaces plagioclase, but it is not abundant in rocks with high Cu content. Minor porphyry style Cu- mineralization occurs in the Cuisson Lake unit and Border phase of the GMB (Fig. 1; Schiarizza, 2015).

Samples

A total of 18 samples were collected for this study including 15 samples from the GMB and three from the Sheridan Creek stock (Table 1). Locations of these samples are shown in Fig. 1 and listed in Table 1 of the Appendix. Detailed descriptions of the samples are provided by Kobylinski et al. (2017).

Table 1. List of samples used for zircon trace element analysis

Mine phase - Mineralized*	GBR-2, GBR-7, GBR-12, GBR-15, GBR-21
Mine phase - Un-mineralized*	GBR-11, GBR-28, GBR-32, GBR2-25, GBR2-26
Granite Mountain phase	GBR2-30, GBR2-38
Border phase	GBR2-15, GBR2-16, GBR2-17
Sheridan Creek stock	GBR2-19, GBR2-23, GBR2-28

** "Mineralized" is defined as samples containing macroscopically visible chalcopyrite grains. "Un-mineralized" samples do not show visible grains of chalcopyrite.*

Analytical methods

Bulk Rock geochemistry

Bulk rock geochemical analysis was carried out at Activation Laboratories (analytical code 4LITHOS). Crushed bedrock samples were analyzed by inductively coupled plasma – mass spectrometry (ICP-MS; Perkin Elmer Sciex ELAN 9000) after a lithium metaborate and lithium tetraborate fusion. Geochemical results are listed in Appendix (Table 2). Analytical precisions, accuracies and a list of reference materials used are listed in the Appendix (Table 2). Loss on ignition was measured at the University of Ottawa using 1-5 grams of pulverized samples at 1050°C for 2 hours.

Zircon

Zircon grains were separated using magnetic and heavy liquid density separation with diiodomethane at a density of 3.3 g/ml. Zircon grains ranging in size from 80 to 350 µm were collected. Grains were handpicked under a binocular microscope, mounted in an epoxy resin and polished to expose centres of grains. Grains of 212-350 µm in size were mounted in three epoxy pucks and the number of zircon grains examined from each sample is listed in the Appendix (Table 3). Zircon grains smaller than 212 µm were mounted in one separate epoxy puck. Grains in epoxy resin were examined under a microscope using transmitted light to verify for the presence of mineral inclusions and fractures. Back scattered electron (BSE) and cathodoluminescence (CL) images were collected for each zircon grain at the University of Ottawa using a JEOL 6610LV scanning electron microscope equipped with CL detector. Since sector-zoned zircon shows highly heterogeneous distribution of elements (Jackson et al., 2013), grains without sector zoning were selected for trace element analysis (Fig. 3).

Laser Ablation Inductively Coupled Plasma Mass Spectrometry (LA-ICP-MS)

LA-ICP-MS analyses were conducted on 232 zircon grains mounted in three epoxy pucks. A NIST 612 (Jochum et al., 2011), 91500 zircon (Wiedenbeck et al., 1995) and a BCR (Jochum et al., 2011), GSEG1 (Jochum et al., 2011) and Plešovice zircon (Sláma et al., 2008) reference material was ablated for every five unknown zircons.

(A)

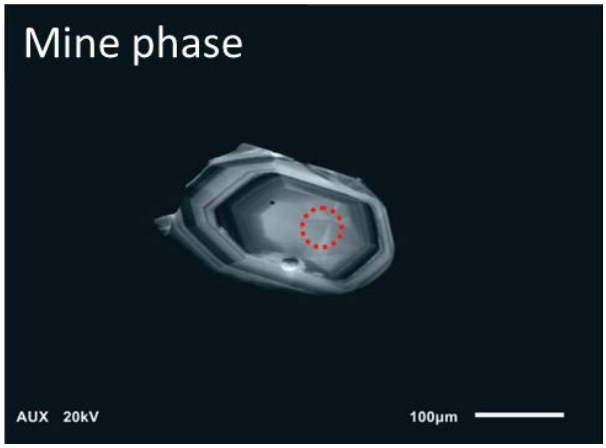

(B)

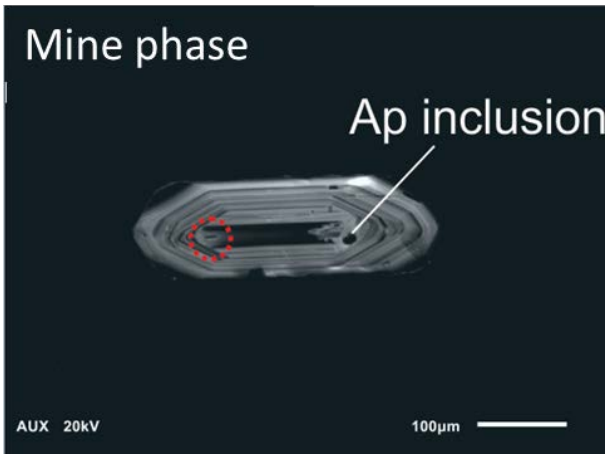

Figure 3. *CL images of zircon from the Mine phase of the GMB showing oscillatory zoning and apatite (Ap) inclusion. The location for laser ablation is shown in red dashed circles. Th/U ratios are 0.18 (A), 0.48 (B)*

U-Pb analysis

Raw count data for U-Pb were reduced using the UPb.age script in the R software environment (Solari and Tanner, 2011). The script reduces data based on accepted values of 91500 zircon (Wiedenbeck et al., 1995). UPb.age eliminates outliers (±2σ), corrects instrument drift using a linear model and corrects for downhole fractionation using a mean method. 2σ uncertainty was used for all age dating when using Isoplot v.4.14 (Ludwig, R. K., 2012) to determine ages. Plešovice zircon was used for validation and to calculate excess variance. Systematic uncertainty ((ratio uncertainty (2σ, S_y) of reference material + excess variance of validation material (2σ, ε') + decay constant error(λ)) was propagated unto population uncertainty (S_x). $^{207}Pb/^{235}U$ systematic error % is 6.8% and $^{206}Pb/^{238}U$ systematic error is 3.4%. Samples analysis were discarded if they were found to be outliers using a weight mean test or if an inclusion was detected by the U.Pb.age script, using ^{140}Ce, ^{31}P,^{42}Ca or ^{56}Fe as proxies for common zircon inclusions (apatite, Fe-oxides).

Trace element analysis

Raw counts for trace elements were reduced using the GLITTER! software (Griffin et al., 2008). Trace elements were calibrated from SiO_2 which was manually entered for each standard (NIST612, GSE1G and BCR2G) using their preferred values (Jochum et al., 2011). SiO_2 was converted to ^{29}Si by the GLITTER! software. NIST612 was used as a primary internal reference/normalizing material (^{29}Si = 72.01) with GSE1G (^{29}Si = 54.4), BCR2G (29Si = 53.7) as secondary standards and zircon 91500 used as validation. Analysis runs with a larger than 10% absolute error between preferred 91500 values for trace elements and determined 91500 values were discarded. Samples analysis were discarded if an inclusion was detected by the GLITTER! software, using ^{31}P,^{42}Ca or ^{56}Fe as proxies for common zircon inclusions (apatite and Fe-oxides).

For a detailed description of error analysis, error propagation and detailed data concerning reference and validation materials, please see Appendix (Table 4). A full report on the metadata for U-Pb and trace element data acquisition is available in the Appendix (Table 6).

Results

Zircon grains

Zircon grains show prismatic faces with length to width ratios ranging from 1 to 3 (Fig. 3). All zircon grains show oscillatory growth zoning (Fig. 3). Most zircon grains contain apatite inclusions (5–30 µm in length; Fig. 3 B) and all but one grain

show a prominent core and rim. Analytical results from one zircon grain were rejected based on the presence of overgrowth of a resorbed core, low Th/U (0.1) and high Nd/Yb (0.027) values. Th/U ratios for the remaining zircon data range from 0.18 to 1.44 and Th concentrations range from 4.9 to 90.5 ppm. Relatively low Th/U ratios in zircon grains reflect low Th in the parental magmas as the concentrations of Th in zircon are positively correlated with a correlation coefficient of 0.74 with those of the bulk rocks (Fig. 4).

U-Pb dates

Magmatic zircon from the mineralized Mine phase show ages ranging from 218.9±3.1 Ma to 201.9 ± 5.0 Ma and three age groups are recognized with time gaps greater than 0.2 m. y. between each one (Table 2). The oldest group is represented by sample GBR-7 and shows an age of 218.9±3.1 Ma. It is followed by a second group with sample GBR-2 at 213.2 ±2.4 Ma. The next youngest group is represented by samples GBR-12 at 206.8 ±4.0 Ma, GBR-15 at 205.9 ±3.7 Ma, GBR-21 at 205.6 ±4.4 Ma and GBR-16 at 201.9 ±5.0 Ma. Ages are calculated using $^{207}Pb/^{235}U$ and $^{206}Pb/^{238}U$ ratios from sample zircons and plotted on a Concordia diagram with appropriate errors (S_x + propagated systematic error). The results plot concordantly on the Concordia diagram and give the ages listed above and below.

Table 2: U-Pb ages from this study

Phase	Samples	MSWD	U-Pb age
Mineralized Mine phase group A	GBR-7 n=16	0.68	218.9±3.1 Ma
Mineralized Mine phase group B	GBR-2 n=27	0.62	213.2 ± 2.4 Ma
Mineralized Mine phase group C	GBR-12 n=11	1.7	206.8 ±4.0 Ma
	GBR-15 n=12	0.84	205.9 ±3.7 Ma
	GBR-16 n=7	0.037	201.9 ±5.0 Ma
	GBR-21 n=9	0.88	205.6 ±4.4 Ma

n: number of zircon grains analyzed
$^{238}U/^{235}U$ ratio = 137.818 (Hiess et al., 2012)

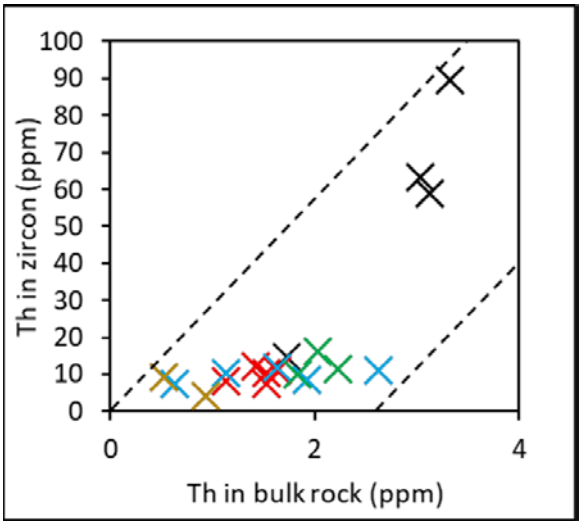

Figure 4. *Compositions of zircon in the GMB and Sheridan Creek stock (black X symbols), Th in zircon vs. Th in bulk rock. The figure shows correlation between Th in bulk rock and Th in zircon with a correlation coefficient of 0.74.A weaker correlation coefficient of 0.55 is present if only samples from the GMB are considered (red = mineralized Mine phase, blue = Un-mineralized Mine phase, green = Border Phase and yellow = Granite Mountain phase, X symbols)*

Rare earth element abundances

Bulk rock

Normalized bulk rock REE patterns show a gentle negative slope with enrichment in light REEs (La_N to Gd_N) ranging from 55 to 196 times chondrite values and HREEs (Tb_N to Lu_N), 46 to 150 times chondrite values. The ratios of La_N/Lu_N vary from 1.84 to 9.8 in the GMB and 3.7-13.6 in the Sheridan Creek stock. The values of Eu/Eu* range from 0.57 to 1.12 for the GMB, and from 0.7 to 1.09 in the Sheridan Creek stock (Fig. 5).

Zircon

Zircon grains contain total concentrations of REEs from 340 to 1433 ppm. All zircon grains show similar chondrite normalized REE patterns with positive Ce anomalies and negative Eu anomalies (Fig. 5). The amplitude of these anomalies varies between different phases.

Cerium anomalies in zircon are calculated using three methods and expressed as Ce^{4+}/Ce^{3+}, Ce/Ce* and Ce/Nd.

Ce^{4+}/Ce^{3+} is calculated following the method of Ballard et al. (2002), which requires REE concentrations of zircon and bulk rock data. The calculation assumes the composition of whole rock to represent parental magma composition. The abundance of Ce^{3+} is determined based on the lattice strain model of Blundy and Wood (1994) for mineral-melt partitioning of elements (Pr, Nd, Sm, Gd, Tb, Dy, Ho, Er, Yb, Lu).

Ce/Ce* values for zircon were calculated using the formula suggested by Loader et al. (2017): ($Ce^* = \frac{(N\,d_N)^2}{Sm_N}$). The advantage of this formula is that it does not require bulk rock composition data.

Ce/Nd is the concentration ratios of Ce to Nd in zircon. Europium anomalies in bulk rock and zircon were calculated using $Eu/Eu^* = Eu_N/(Sm_N * Gd_N)^{1/2}$ as utilized by Dilles et al. (2015) and Lee et al. (2017) amongst others.

Mean and median values of Ce^{4+}/Ce^{3+}, Ce/Ce*, Ce/Nd, and Eu/Eu*, and the number of samples analyzed for the different intrusions are presented in Table 3 and depicted in Figs. 6, 7, 8, and 9. In summary, samples from the mineralized Mine phase have the highest average Ce^{4+}/Ce^{3+} and Ce/Ce* values compared to the other intrusive phases in the GMB and the Sheridan Creek stock (Fig. 6). The mineralized Mine phase has the highest Ce/Nd ratios compared to the other phases of the GMB, but the Sheridan Creek stock has the highest average Ce/Nd ratio (Fig. 8). The Mineralized Mine phase, Un-mineralized Mine phase and Border phase have lower Eu/Eu* in zircon compared to the Granite Mountain phase and Sheridan Creek stock (Fig. 9).

Discussion

Ages of the GMB

GMB is a large batholith with the surface exposure of 15 km wide by 20 km long.

Combined with the available ages, this study shows that the batholith formed through several pulses of intrusions over a time span of 20 million years. In chronological order, the available ages of intrusions in the GMB are as follows. The oldest age is reported from two samples of the Burgess Creek stock, which is composed of tonalites and quartz diorites (Schiarizza, 2015). It is dated at 222.71±0.22 Ma for the tonalites and 221.25±0.2 Ma for the quartz diorite (Schiarizza, 2015). These ages are similar to tonalite sample GBR-7, in the mineralized Mine phase, 218.9±3.1 Ma, obtained in this study (Appendix, Table 4, Figs. 2 and 6). One leucocratic tonalite sample from the Granite Mountain phase yielded 217.15±0.2 Ma (Fig. 2) (Schiarizza, 2015). Our results combined with the ones of Schiarizza (2015) suggest that the Burgess Creek stock is 2-5 Ma older than the other phases of the GMB. As suggested by Ash et al. (1999a, b), the Burgess Creek stock could be considered as an old border phase of the GMB. The remaining mineralized Mine phase samples (n=5) reveal two additional groups of ages (Table 4 of the Appendix, Figs. 2 and 6); 213.2 ± 2.4 Ma from foliated medium grained tonalites with 20-25 vol.% mafic minerals and 205.8 ±2.1 Ma from foliated medium grained tonalites with 20-30 vol.% mafic minerals.

Table 3: Zircon cerium and europium anomalies

Phase		**Ce^{4+}/Ce^{3+}**	**Ce/Ce***	**Ce/Nd**	**Eu/Eu***
Mineralized	Range	59-1780	15-459	2-17	0.26-0.34
Mine phase	Mean	681	119	8	0.3
group A	Median	714	91	6	0.3
n=15					
Mineralized	Range	41-563	10-181	2.6-35.3	0.27-0.38
Mine phase	Mean	259	67	13.4	0.3
group B	Median	152	47	11.6	0.3
n=14					
Mineralized	Range	21-574	10-294	2.1-28.6	0.18-0.39
Mine phase	Mean	193	82	9.7	0.28
group C	Median	165	70	8	0.28
n=43					
Un-mineralized	Range	9-555	2.6-274	1.3-17.2	0.18-0.47
Mine phase	Mean	103	60.5	8.4	0.3
n=21	Median	77	53	8	0.3
Border phase	Range	14-398	3-162	2.3-25	0.21-0.39
n=28	Mean	115	59	9	0.28
	Median	103	53.7	9	0.28
Granite	Range	43-583	19-196	3.4-22.3	0.24-0.59
Mountain phase	Mean	212	75.5	10.5	0.47
n=21	Median	207	61.1	9.3	0.48
Sheridan Creek	Range	50-355	16.3-112.9	5-23	0.41-0.69
stock	Mean	203	61.2	13.1	0.57
n=28	Median	230	64.6	14	0.58

n=number of zircon grains analyzed

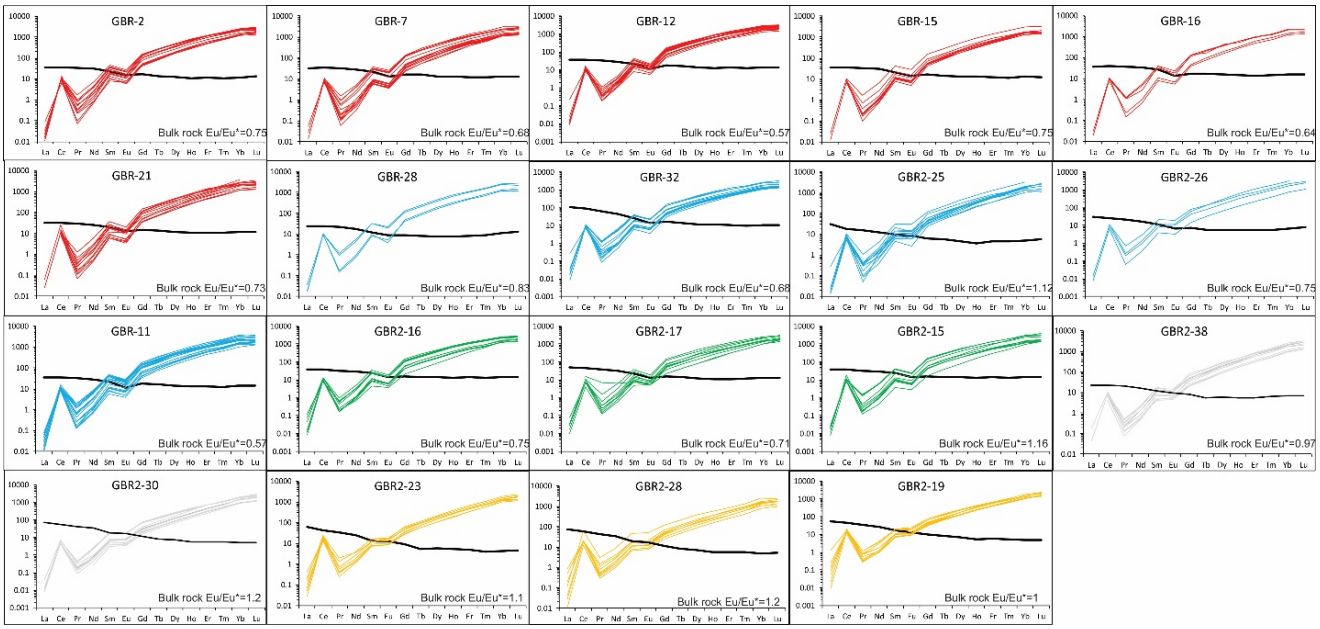

Figure 5. *Chondrite normalized REE patterns for zircon and associated bulk rock. Red patterns are from the mineralized Mine phase, blue from the un-mineralized Mine phase, green from the Border phase, yellow from the Sheridan Creek stock and grey from the Granite Mountain phase. Black lines are chondrite normalized REE patterns of corresponding bulk rock. Eu/Eu* derived from bulk rock is indicated in each plot. Chondrite values after McDonough and Sun (1995).*

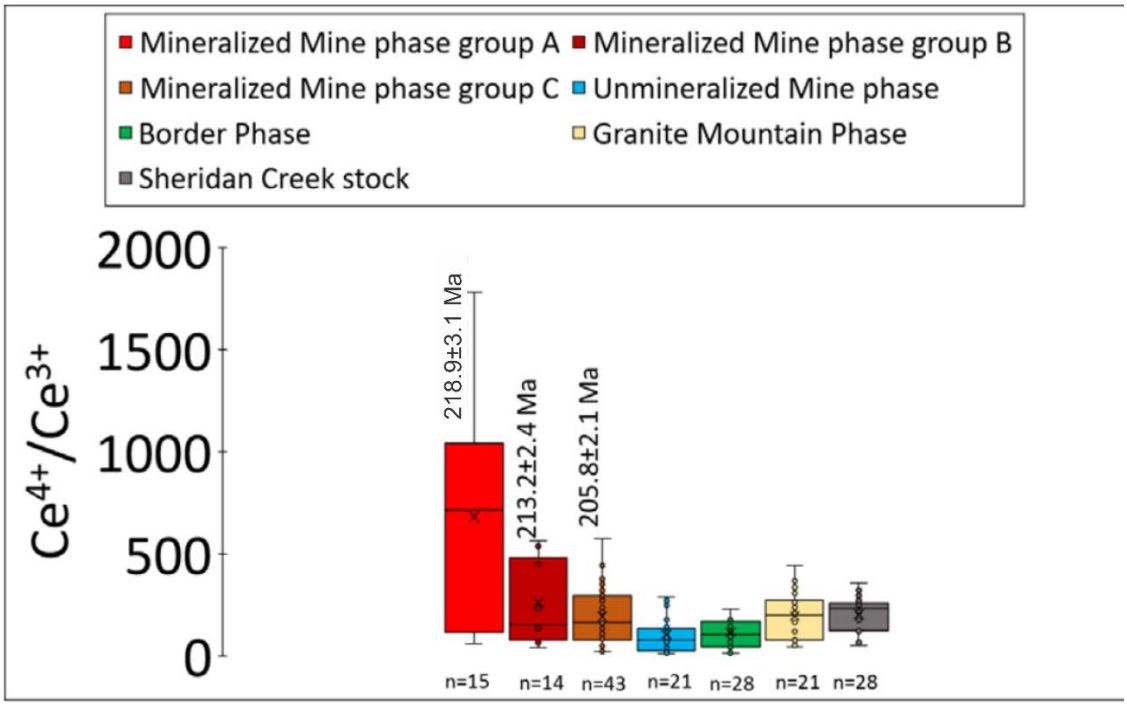

Figure 6. *Box and whisker plots of all Ce^{4+}/Ce^{3+} values in zircon from all samples. Ce^{4+}/Ce^{3+} is calculated using the method proposed by Ballard et al. (2002). X represents the mean value for each plot. Above plots from the mineralized Mine phase intrusions are U-Pb ages. Mineralized Mine phase A, B, and C represent the three age groups defined in our study.*

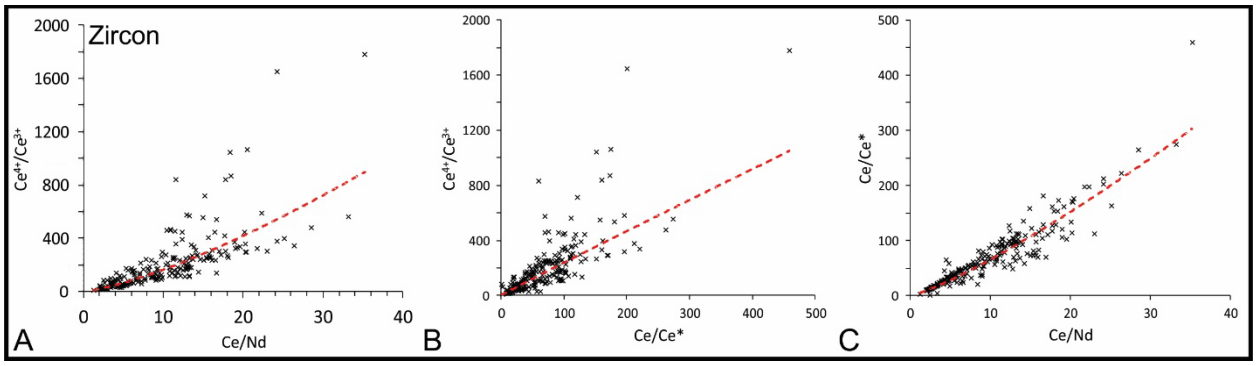

Figure 7. *(A) Ce^{4+}/Ce^{3+} vs. Ce/Nd in zircon graph, correlation coefficient is 0.90 for the following equation: $Ce/Nd = 7.28(Ce^{4+}/Ce^{3+})^{(1.35)}$. (B) Ce^{4+}/Ce^{3+} vs. Ce/Ce* in zircon graph, correlation coefficient is 0.84 for the following equation: $Ce^{4+}/Ce^{3+} = 2.71\ (Ce/Ce^*)^{0.92}$. (C) Ce/Ce* vs. Ce/Nd in zircon graph, correlation coefficient is 0.94 for the following equation: $Ce/Nd = 3.94(Ce/Ce^*)^{(1.21)}$.*

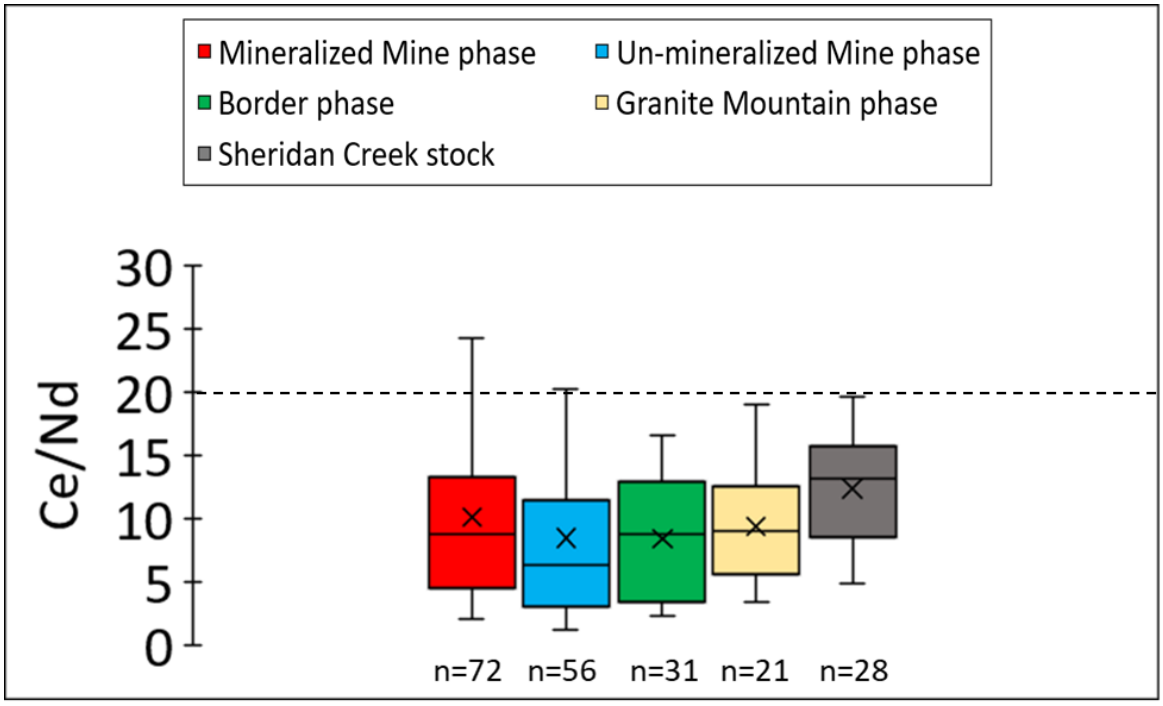

Figure 8. Box and whisker plots of all Ce/Nd values in zircon from all samples. X represents the mean value for each plot. The dashed line shows a Ce/Nd of 20, only samples from the Mine Phase have zircon with values over 20.

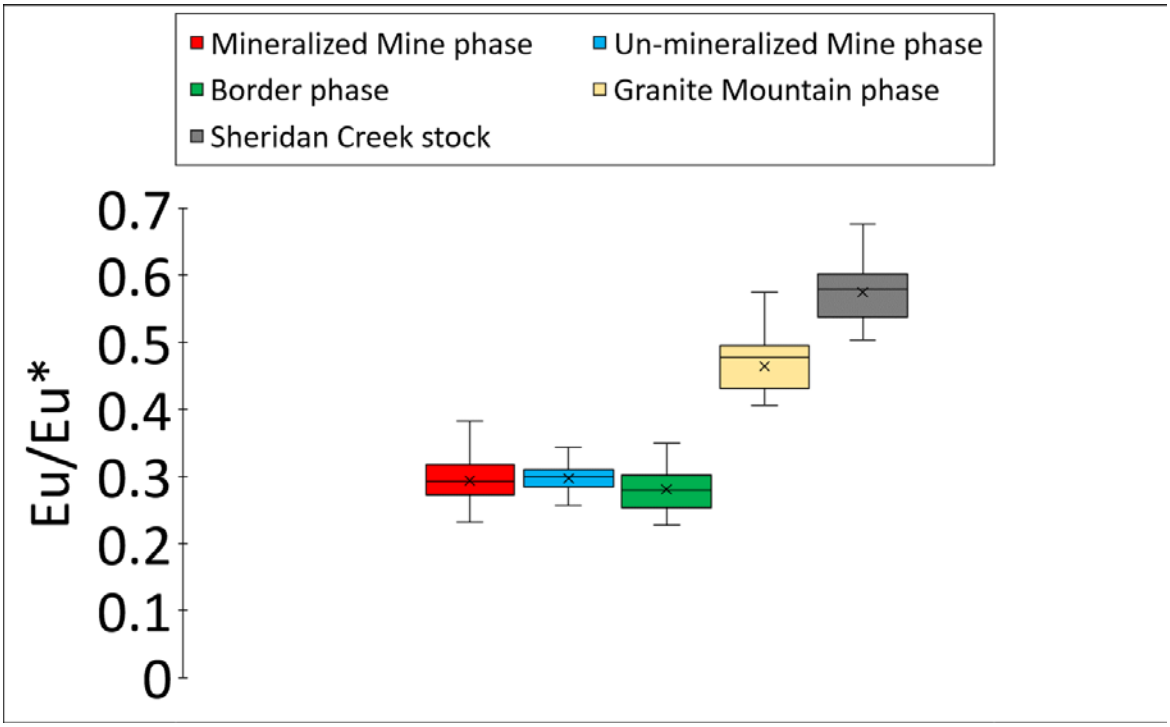

Figure 9. Box and whisker plots of all Eu/Eu* values in zircon from all samples. X represents the mean value for each plot.

Mine phase of the GMB

The Mine phase is composed of foliated tonalite and contains Cu mineralization at its center. This study shows that the Mine phase is made up of three pulses of intrusion (Table 2) with varying ages and Ce^{4+}/Ce^{3+} ratios. Therefore, it was not formed from a single magma.

Many porphyry deposits worldwide are associated with multiple injections of oxidized intrusions focused at the sites of mineralization (Hattori and Keith, 2001; Sillitoe, 2010). This study shows at least 3 groups of intrusions in the mineralized Mine phase. Although the ages are different, their mineralogy and textures are essentially identical making field distinction of the different intrusive phases impractical. All are foliated tonalites with minor variation in SiO_2 wt. % in bulk rock ranging from 65 to 67 wt.% (Table 2 of the Appendix). All have similar mafic mineral modality of chloritized hornblende and biotite, ranging from 20 to 30 vol.%.

The content of Cu in bulk rocks for the mineralized Mine phase intrusions is high, ranging from 120 to 4900 ppm, reflecting the occurrence of visible chalcopyrite. The oldest of these Cu-mineralized intrusions (GBR-7) shows the highest Ce anomalies (median Ce^{4+}/Ce^{3+} = 714). The second and third intrusions from the mineralized Mine Phase show moderately high Ce anomalies (median Ce^{4+}/Ce^{3+}=152 and median Ce^{4+}/Ce^{3+}=165 respectively).

Harding (2012) reported Re-Os ages on molybdenite from the Granite Lake pit (215.0 ± 1.0 Ma and 212.7 ± 0.9 Ma), and the Gibraltar East pit (210.1 +/- 0.9 Ma). Large age ranges suggest multiple mineralization events or recrystallization of molybdenite. The molybdenite ages from Granite Lake pit are similar to the second intrusion of the mineralized Mine phase in this study. This intrusion sample

(GBR-2) was collected close to the Granite Lake pit, suggesting a genetic relationship between this intrusion and the mineralization or recrystallization of molybdenite during the intrusion.

Other nearby deposits

Several porphyry copper deposits are hosted in granitic batholiths that intrude the Nicola volcanic group in the southern part of the Quesnel terrane of the Canadian Cordillera. They include Mount Polley (Cu-Au porphyry deposit), Woodjam (Cu-Mo-Au porphyry prospect), Gibraltar and Highland Valley Copper (Cu-Mo porphyry deposit). The largest among the four is the Highland Valley Copper deposit hosted in the Guichon Creek batholith. The Guichon Creek batholith is 235 km south east of the Gibraltar deposit and intrudes the Nicola Group mafic volcaniclastics (D'Angelo et al., 2017). The mineralized Mine phase group C (201.9 ±5.0 Ma to 206.8 ±4.0 Ma) is similar in age to the Cu-mineralized rocks of the Guichon Creek batholith, that is the Bethsaida, Skeena and Bethlehem facies dated at 208.81±0.21 Ma, 208.3±1.0 Ma and 209.17±0.54 Ma, respectively (D'Angelo et al., 2017). Molybdenite from a quartz molybdenite vein in the Highmont pit of the Highland Valley Copper deposit yielded a Re-Os age of 208.4±0.9 Ma (D'Angelo et al., 2017) which can be considered synchronous with the Cu mineralization and similar to our observation at Gibraltar.

Ce^{4+}/Ce^{3+} values for zircons from chalcopyrite-bearing samples in the Gibraltar deposit are within the range of values (40-700) found in zircons from the Bethsaida Phase and Bethlehem Phase which host Cu-mineralization at the Highland Valley Copper deposit. Samples from the later barren Gnawed Mountain porphyry at Highland Valley show lower Ce^{4+}/Ce^{3+} in zircons (~20-300; Ward, 2008). Our results show that the post-mineralization decrease of Ce^{4+}/Ce^{3+} values in zircon is a common attribute to the Gibraltar and Highland Valley Copper deposits.

Oxidized intrusions in the Mine phase

Porphyry-Cu deposits are associated with subduction related oxidized magmas (Ishihara, 1977; Sillitoe, 2010, Dilles et al., 2015). This is consistent with the higher capacity of oxidized magmas to transport metals and S from the mantle to shallow crustal levels (Hattori and Keith, 2001; Richards, 2003; Cooke et al., 2005; Sillitoe, 2010). The magnitude of Ce^{4+}/Ce^{3+} is linked to the oxidation state of a magma (Shen et al., 2015; Burnham and Berry, 2012; Trail et al., 2012). Ce^{4+}/Ce^{3+} of > 120 for zircon from granitic intrusions forming various deposits in the Central Asian Orogenic Belt are associated with intermediate (1.5 – 4 Mt Cu) and large (>4 Mt Cu) tonnage porphyry-Cu deposits (Shen et al., 2015). Mineralized Mine phase samples show mean and median Ce^{4+}/Ce^{3+}>120 (305 and 172 respectively) confirming the correlation between intrusion porphyry mineralization fertility with elevated Ce^{4+}/Ce^{3+} ratios (ca. >120).

Sample GBR-7, which yielded the oldest age in the mineralized Mine phase, shows the highest Ce^{4+}/Ce^{3+} values in zircon in this study (Fig. 6). Zircons from younger intrusions in the mineralized Mine phase show lower Ce^{4+}/Ce^{3+}, but the values are still higher than those for zircons from unmineralized intrusions in the Mine phase and other phases of the GMB (Fig. 6).

Implications for exploration

Cerium anomalies in zircon are evaluated three ways in this study: Ce^{4+}/Ce^{3+}, Ce/Ce*and Ce/Nd. All Ce anomalies are positively correlated with correlation coefficient >0.8 (Fig. 7). The data suggests that Ce/Nd or Ce/Ce* may be used to evaluate Ce^{4+}/Ce^{3+} in zircon. For instance, Chelle-Michou et al. (2014) used Ce/Nd in zircon to differentiate oxidized porphyritic rocks (Ce/Nd; 9-46) from reduced gabbronorite host rocks (Ce/Nd; 2-12) in the Coroccohuayco porphyry deposit, Peru.

A number of studies suggested that detrital zircon from stream sediments or till could be used to test the porphyry potential of a poorly exposed intrusion (e.g. Ballard et al., 2002; Dilles et al., 2015; Hattori et al., 2016; Lu et al., 2016; Plouffe and Ferbey, 2017). Our correlation results between the three Ce anomalies (Ce^{4+}/Ce^{3+}, Ce/Ce*and Ce/Nd) further demonstrate that Ce/Nd or Ce/Ce* can be calculated using detrital zircons (as oppose to Ce^{4+}/Ce^{3+} which require the bulk rock composition) as a proxy for oxidation conditions and the porphyry fertility potential of an intrusion.

Wolfe (2017) and Wolfe et al. (2017) report the composition of 45 zircon grains recovered from five till samples strategically located up- and down-ice from mineralization (Fig. 10). Only one till sample located <1 km to the west (down-ice) of the Gibraltar East pit (11PMA024A02 in Fig. 10) contains two zircon grains with a Ce/Nd ratio >20 corresponding to the highest Ce/Nd values measured in the mineralized Mine phase in this study. A third zircon grain from the same till sample has a Ce/Nd of 19 corresponding to the high values in the mineralized and unmineralized Mine phase (see also Plouffe et al., 2018). These results suggest that detrital zircon grains from till with Ce/Nd > 20 are derived from and indicative of a mineralized porphyry system. Given that zircon composition is robust and is not easily affected by secondary or alteration processes, our results demonstrate that Ce/Nd or Ce/Ce* in detrital zircons can be used to identify buried undiscovered porphyry-Cu deposits. However, more testing of zircon composition in detrital sediments in the region of porphyry deposits is required.

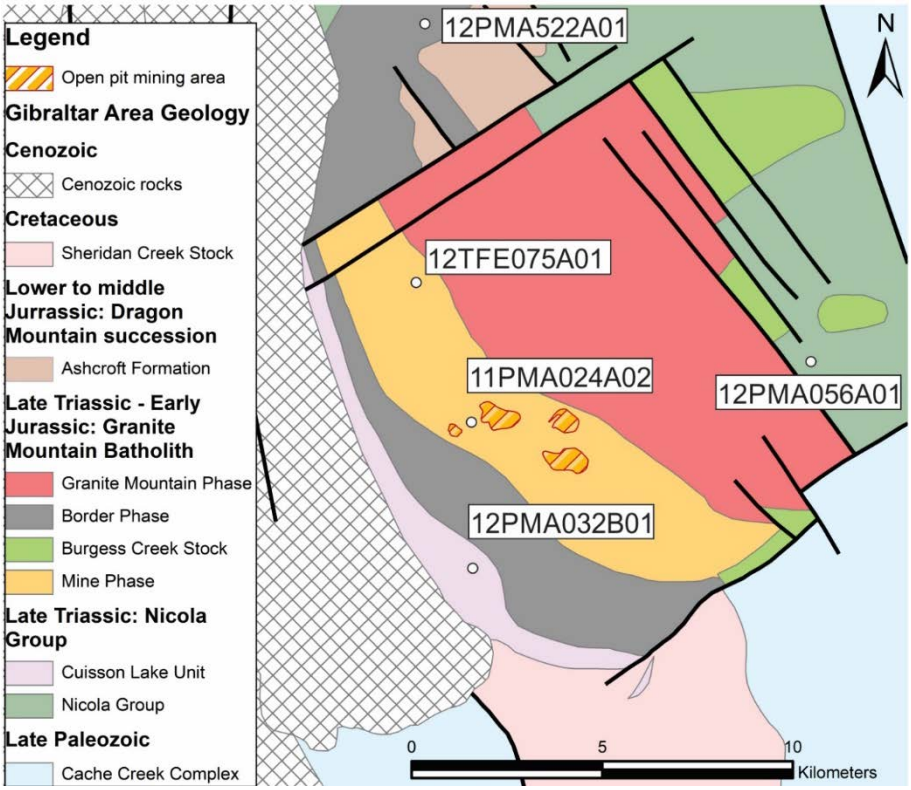

Figure 10. *Location of till samples from which zircon grains were analyzed by LA-ICP-MS by Wolfe (2017).*

Summary

The GMB is a composite batholith containing multiple pulses of intrusions separated by time and space. Zircons indicative of oxidizing conditions with mean Ce^{4+}/Ce^{3} ratio of 305 crystalized from the mineralized Mine phase of GMB at ~219 Ma. This was followed by two intrusive pulses at ca. 213 and 205 Ma, having contributed additional Cu-mineralization or remobilized previous Cu-mineralization at Gibraltar. Molybdenum was introduced in the system during the 213 Ma event as suggested by Re-Os ages of 210-215 Ma on molybdenite from the mineralized Mine phase (Harding, 2012).

Ce/Nd and Ce/Ce* measured in detrital zircon grains could be used in mineral exploration to detect buried or poorly exposed potentially fertile intrusion. At Gibraltar, till zircon grains with Ce/Nd > 20 most likely corresponding to the mineralized Mine phase, were only found in a sample <1 km down-ice from mineralization.

Acknowledgements

This project was made possible through a Research Affiliate Program (RAP) bursary to CHK. We thank Bill Davis from the Geological survey of Canada for his review and constructive comments concerning LA-ICP-MS data acquisition, error analysis and data processing. We also thank Samuel Morfin and Duane Petts at the University of Ottawa's LA-ICP-MS laboratory for their expertise and advice during LA-ICP-MS analysis of zircon. We also thank Glenn Poirier at the University of Ottawa for his expertise and help with taking CL images of zircons. This study is part of the porphyry-style mineral system project of the Targeted Geoscience Initiative-5 (TGI-5) Program of the Geological Survey of Canada.

References

Ash, C.H., Panteleyev, A., MacLellan, K.L., Payne, C.W., and Rydman, M.O., 1999a. Geology of the Gibraltar Mine area (93B/6&9); British Columbia Ministry of Energy and Mines, Open File 1999-7, scale 1:50 000.

Ash, C. H., Rydman, M. O., Payne, C. W., and Panteleyev, A., 1999b. Geological setting of the Gibraltar Mine, South Central British Columbia (93B/93A); *in*: Exploration and mining in British Columbia 1998., British Columbia Ministry of Energy and Mines, p. A1–A15.

Ash, C. H., and Riveros, C. P., 2001. Geology of the Gibraltar copper-molybdenite deposit, east-central British Columbia (93B/9); *in*: Geological Fieldwork 2000. British Columbia Ministry of Energy and Mines, Victoria, Paper, 1, p. 119-134.

Ballard, J R., Palin, M. J., and Campbell, I.H., 2002. Relative oxidation states of magmas inferred from Ce (IV)/Ce (III) in zircon: application to porphyry copper deposits of northern Chile; Contributions to Mineralogy and Petrology, 144.3: p. 347-364.

Blundy, J., and Wood, B., 1994. Prediction of crystal–melt partition coefficients from elastic moduli. Nature, 372(6505), p. 452.

Burnham, A. D., and Berry, A. J,. 2012. An experimental study of trace element partitioning between zircon and melt as a function of oxygen fugacity; Geochimica et Cosmochimica Acta, 95: p. 196-212.

Bysouth, G.D., Campbell, K.V., Barker, G.E., and Gagnier, G.K., 1995. Tonalite-trondhjemite fractionation of peraluminous magma and the formation of syntectonic porphyry copper mineralization, Gibraltar mine, central British Columbia; *in*: Schroeter, T.G. (Ed.), Porphyry deposits of the northwestern cordillera of North America, Canadian Institute of Mining, Metallurgy and Petroleum, Special Volume 46, p. 201-213.

Chelle-Michou, C., Chiaradia, M., Ovtcharova, M., Ulianov, A., and Wotzlaw, J. F,. 2014. Zircon petrochronology reveals the temporal

link between porphyry systems and the magmatic evolution of their hidden plutonic roots (the Eocene Coroccohuayco deposit, Peru); Lithos, 198, p. 129-140.

Cooke, D. R., Peter H., and John L. Walshe,. 2005. Giant porphyry deposits: characteristics, distribution, and tectonic controls; Economic Geology, 100.5: p. 801-818.

D'Angelo, M., Miguel, A., Hollings, P., Byrne, K., Piercey, S., and Creaser, R. A,. 2017. Petrogenesis and Magmatic Evolution of the Guichon Creek Batholith: Highland Valley Porphyry Cu±(Mo) District, South-Central British Columbia; Economic Geology, 112(8), p. 1857-1888.

Dilles, J. H., Kent, A. J. R., Wooden, J. L., Tosdal, R. M., Koleszar, A., Lee, R. G., and Farmer, L.P., 2015, Zircon compositional evidence for sulfur-degassing from ore-forming arc magmas; Economic Geology, v. 110, p. 241–251.

Drummond, A.D., Sutherland Brown, A., Young, R.J., and Tennant, S.J., 1976. Gibraltar – regional metamorphism, mineralization, hydrothermal alteration and structural development; *in:* Sutherland Brown, A. (Ed.), Porphyry deposits of the Canadian Cordillera, Canadian Institute of Mining and Metallurgy, Special Volume 15, p. 195-205

Griffin, W. L., Powell, W. J., Pearson, N. J., and O'reilly, S. Y,. 2008. GLITTER: data reduction software for laser ablation ICP-MS. Laser Ablation-ICP-MS in the earth sciences; Mineralogical association of Canada short course series, 40, p. 204-207.

Harding, B,. 2012. The characterization of molybdenum mineralization at the Gibraltar mines Cu-Mo porphyry, central British Columbia; B. Sc. thesis, Queen's University, 52p.

Hartmann, L. A., and Santos, J. O. S,. 2004. Predominance of high Th/U, magmatic zircon in Brazilian Shield sandstones; Geology, 32(1), p. 73-76.

Hattori, K., and Keith, J. D., 2001. Contribution of mafic melt to porphyry copper mineralization: evidence from Mount Pinatubo, Philippines, and Bingham Canyon, Utah, USA; Mineralium Deposita, 36.8: p. 799-806.

Hattori, K., Morfin, S., Baumgartner, R., Shen, P., and Petts, D., 2016. Fertility of igneous rocks related to porphyry copper deposits: indications from zircon compositions; XVIII Peruvian Geological Congress, p. 3

Hiess, J., Condon, D. J., McLean, N., & Noble, S. R., 2012. 238U/235U systematics in terrestrial uranium-bearing minerals; Science, 335(6076), p. 1610-1614.

Ishihara, S., 1977. The magnetite-series and ilmenite series granitic rocks; Mining Geology, v. 27, p. 293–305

Jackson, S. E., Dube, B., Chapman, J., and Gao-J-F,. 2013. Applications of LA-ICP-MS element mapping in mineral deposit research and exploration: mineral deposit research for a high-tech world; 12th SGA Biennial Meeting, Uppsala, Sweden, 2013, Proceedings, v. 1, p. 201–204

Jochum, K. P., Weis, U., Stoll, B., Kuzmin, D., Yang, Q., Raczek, I., and Günther, D,. 2011. Determination of reference values for NIST SRM 610–617 glasses following ISO guidelines; Geostandards and Geoanalytical Research, 35(4), p. 397-429.

Kobylinski, C., Hatori, K., Smith, S., and Plouffe, A., 2016. Report on the composition and assemblage of minerals associated with the porphyry Cu-Mo mineralization at the Gibraltar deposit, south central British Columbia, Canada; Geological Survey of Canada, Open File 8025, 30 p.

Kobylinski, C H., Hattori, K., Plouffe, A., and Smith, S W,. 2017. Epidote associated with

the porphyry Cu-Mo mineralization at the Gibraltar deposit, south-central British Columbia; Geological Survey of Canada, Open File 8279, https://doi.org/10.4095/305912

Lee, R.G., Dilles, J.H., Tosdal, R.M., Wooden, J.L., and Mazdab, F.K., 2017. Magmatic evolution of granodiorite intrusions at the El Salvador porphyry copper deposit, Chile, based on trace element composition and U/Pb age of zircons; Economic Geology, v. 112, p. 245-273, doi:10.2113/econgeo.112.2.245

Liang, H. Y., Campbell, I. H., Allen, C., Sun, W. D., Liu, C. Q., Yu, H. X., and Zhang, Y. Q,. 2006. Zircon Ce $^{4+}$/Ce^{3+} ratios and ages for Yulong ore-bearing porphyries in eastern Tibet; Mineralium Deposita, 41(2), p. 152.

Lu, Y.-J., Loucks, R.R., Fiorentini, M., McCuaig, T.C., Evans, N.J., Yang, Z.-M., Hou, Z.-Q., Kirkland, C.L., Parra-Avila, L.A., and Kobussen, A., 2016. Zircon composition as a pathfinder for porphyry Cu ± Mo ± Au deposits; *in* Tectonics and metallogeny of the Thetyan Orogenic Belt; *in*: Society of Economic Geologists, Special Publication No. 19, Littleton, Colorado, p. 329-347.

Ludwig, R. K., 2012. Isoplot 4.15 A geological toolkit for Microsoft Excel; *in*: Berkeley Geochronology Center Special Publication No. 5.

McDonough, W. F,. Sun S,. 1995. The composition of the Earth; Chemical Geology 120: p. 223-253

Oliver, J., Crozier, J., Kamionko, M., and Fleming, J., 2009. The Gibraltar Mine, British Columbia. A billion tonne deep copper-molybdenum porphyry system: structural style, patterns of mineralization and rock alteration; Association for Mineral Exploration British Columbia, 2009 Mineral Exploration Roundup, Vancouver, BC, Abstracts, p. 35-36.

Panteleyev, A., 1978. Granite Mountain project (93B/8); Geological Fieldwork 1977, British Columbia Ministry of Energy, Mines and Petroleum Resources, British Columbia Geological Survey Paper 1977-1, p. 39-42.

Plouffe, A., and Ferbey, T,. 2015. Till composition near Cu-porphyry deposits in British Columbia: Highlights for mineral exploration; *in*: TGI 4 - Intrusion Related Mineralization Project: New Vectors to Buried Porphyry-Style Mineralization. Geological Survey of Canada, Open File 7843, p. 15-37.

Plouffe, A. and Ferbey, T., 2017. Porphyry Cu indicator minerals in till: A method to discover buried mineralization; *in:* Indicator Minerals in Till and Stream Sediments of the Canadian Cordillera, (eds.) T. Ferbey, A. Plouffe, and A. Hickin; Mineral Association of Canada, Topics in Mineral Sciences Volume 47, Geological Association of Canada, Special Paper 50, p. 129-159.

Plouffe, A., Kobylinski, C.H., Hattori, K., Wolfe, L., and Ferbey, T., 2018. Mineral markers of porphyry copper mineralization: Work in progress at the Gibraltar deposit, British Columbia; *in* Targeted Geoscience Initiative - 2017 Report of Activities: Volume 1, (ed.) N. Rogers; Geological Survey of Canada, Open File 8358, p. 59-69.

Richards, J. P,. 2003. Tectono-magmatic precursors for porphyry Cu-(Mo-Au) deposit formation; Economic Geology 98.8: p. 1515-1533.

Schiarizza, P., 2014. Geological setting of the Granite Mountain batholith, host to the Gibraltar porphyry Cu-Mo deposit, south-central British Columbia in Geological Fieldwork 2013, British Columbia Ministry of Energy and Mines, British Columbia Geological Survey, Paper 2014-1, p. 95-110.

Schiarizza, P,. 2015. Geological setting of the Granite Mountain batholith, south-central British Columbia; Geological Fieldwork

2014, British Columbia Ministry of Energy and Mines, British Columbia Geological Survey Paper, p. 19-39.

Shen, P., Hattori, K., Pan, H., Jackson, S., & Seitmuratova, E,. 2015. Oxidation condition and metal fertility of granitic magmas: zircon trace-element data from porphyry Cu deposits in the Central Asian Orogenic Belt; Economic Geology, 110(7), p. 1861-1878.

Sillitoe, R. H., 2010. Porphyry copper systems; Economic geology v.105.1 p. 3-41.

Solari, L. A., and Tanner, M,. 2011. UPb. age, a fast data reduction script for LA-ICP-MS U-Pb geochronology; Revista Mexicana de Ciencias Geológicas p. 28

Sláma, J., Košler, J., Condon, D. J., Crowley, J. L., Gerdes, A., Hanchar, J. M., and Schaltegger, U., 2008. Plešovice zircon—a new natural reference material for U–Pb and Hf isotopic microanalysis. Chemical Geology, 249(1-2), p. 1-35.

Sutherland Brown, A,. 1976. Morphology and classification. Porphyry deposits of the Canadian Cordilleran; *in*: Canadian Institute of Mining and Metallurgy Special, 15, p. 44-51.

Trail, D., Watson, E. B., and Tailby, N. D,. 2012. Ce and Eu anomalies in zircon as proxies for the oxidation state of magmas; Geochimica et Cosmochimica Acta, 97, p. 70-87.

van Straaten, B.I., Oliver, J., Crozier, J., and Goodhue, L., 2013. A summary of the Gibraltar porphyry copper-molybdenum deposit, south-central British Columbia, Canada. *in*: Logan, J. and Schroeter, T. G. (Eds.), Porphyry systems of central and southern BC: Prince George to Princeton, Society of Economic Geologists Field Trip Guidebook 43, p. 55-66.

Ward, R. S,. 2008. Isotope geochemistry of zircon from the Guichon batholith, Highland Valley copper deposit: southern British Columbia: Relationship between Ce^{4+}/Ce^{3+} in zircon, oxidation state in magmas and ore genesis; B.Sc thesis, submitted to the faculty of earth sciences, Carlton University, Ottawa, Canada.

Wolfe, L., 2017. Chemistry of refractory indicator minerals in tills around the Gibraltar porphyry copper deposit, southcentral British Columbia; unpublished B.Sc. thesis, University of Ottawa, Ottawa, 56 p.

Wolfe, L., Hattori, K., and Plouffe, A., 2017. Glacial dispersal of refractory minerals from the Gibraltar porphyry copper deposit, south central British Columbia, Canada; Geological Survey of Canada, Scientific Presentation 73, https://doi.org/10.4095/305829

Wiedenbeck M., Allé P., Corfu F., Griffin W. L, Meier M., Oberli F., von Quadt A., Roddick J.C., and Spiegel W,. 1995. Three natural Zircon standards for U-Th-Pb, Lu-Hf, trace element and REE analyses; Geostandards Newsletter, 19 (1) p. 1-23

Appendix

See attached file: Appendix.xlsx

Table 1. GPS locations for samples used in this study. Coordinates are in NAD 83, Zone 10 N

Table 2. Accuracies, precisions, detection limits and bulk rock compositions of samples

Table 3. Trace element concentrations in zircon

Table 4. U-Pb age dating and data on validation materials (combined results and results separated by samples are presented into two sheets).

Table 5. Concordia diagrams

Table 6. Detailed metadata for LA-ICPMS analysis runs